

ESTIMATING THE FATIGUE RELIABILITY OF HYDRAULIC TURBINE RUNNER BLADES USING FRAILTY MODELS AND CENSORED MAINTENANCE DATA

Theophile Mbuyi Tshibangu^{1*}, Guyh Dituba Ngoma¹, Martin Gagnon²,

¹School of Engineering, University of Quebec in Abitibi-Témiscamingue, Rouyn-Noranda, Canada

²Institut de Recherche d'Hydro-Québec, Varennes, Canada

*theophilembuyi.tshibangu@uqat.ca

Abstract—Hydropower plays a critical role in the global energy transition. The hydraulic turbine runner, a key component of the turbine-generator unit, is susceptible to two forms of damage: cavitation and fatigue. Despite continuous monitoring systems equipped with sensors to measure key operating parameters, these systems are unable to detect cracks in turbine runner blades. Consequently, such cracks are often unexpectedly discovered during planned maintenance. Turbine blade cracking is a rare event leading to right-censored observations during inspections. Hence survival frailty models can be used to account for both censored data and variability observed among individuals within the same family. Maintenance data analyzed in this study are collected from inspections and repairs of 18 turbine runners. By incorporating the frailty effect to account for heterogeneity within a family, the results suggest that some turbines exhibit similar reliability patterns. Model fit is assessed using the chi-square test, confirming acceptability at a 95% significance level. Additionally, the root mean squared error is used to evaluate model accuracy and to compare the cumulative hazard function to a non-parametric Nelson-Aalen estimator. The confidence interval for the cumulative hazard function is evaluated at a 95% confidence level, using the delta method to quantify the uncertainty resulting from the estimation of model parameters. Despite the limited data, the frailty model outperforms the Nelson-Aalen estimator. Optimizing model parameters with a robust algorithm using right-censored data suggests that crack events in hydraulic turbine runner blades appear to follow a frailty model.

Keywords-component—Reliability; Frailty Models; Maintenance Data; Cracking; Hydraulic Turbine.

I. INTRODUCTION

The energy transition requires effective monitoring of equipment used to produce green energy [1]. In hydroelectric power generation, the turbine runner is a critical component. Ensuring its availability demand an optimized maintenance strategy to mitigate major damages, particularly cavitation and blade cracking [2]. Figure 1 illustrates the crack observed on a Francis turbine with a diameter of 5.740 meters.



Figure. 1. Cracks on Francis runner blade.

The complexity of fluid dynamics during start-up and shut-down cycles presents significant challenges for researchers in accurately assessing dynamic load spectra to predict cracking events [3]. Stress fluctuations in transient regimes require a comprehensive understanding of their effects on turbine runner blades [4]. On-site experiments can be conducted to observe stress distributions on turbine blades [5]. However, these measurements are costly and require extensive sensor installation. While monitoring systems facilitate the measurement of key operating parameters, they remain incapable of detecting or accurately predicting cracks in turbine runner blades.

Over the years, data-driven methods have been developed to estimate the service life of repairable components, offering new insights into predictive maintenance and reliability assessment [6]. These methods aim to provide a more accurate prognosis of the variable of interest. In the case of hydraulic

turbine blade cracking, historical maintenance data are frequently right-censored. In some instances, the occurrence of cracks is very spaced out, due to long inspection intervals, resulting in limited data for analysis. Given the variability in crack occurrence among components of the same family operating under similar conditions, survival frailty models offer a means to account for this heterogeneity. These models offer the advantage of incorporating an individuality factor for each component, accounting for potential differences such as casting defects, installation errors, welding defects, and other variations [8]. In addition, they enable the correlation of explanatory variables.

II. FRAILTY MODELS

For repairable entities under the minimal repair assumption, the non-homogeneous Poisson process (NHPP) is widely used in the literature [9], [10]. The minimal repair assumption considers that the repair (such as welding of cracks) merely restores the entity to its prior bad condition (as bad as old). The most used failure intensity function in NHPP is the power law [10], defined in (1).

$$h_0(t) = \omega \rho t^{\rho-1} \quad (1)$$

where ω is the scale parameter and ρ is the shape parameter of the curve.

If $\rho > 1$, the system is deteriorating (sad system),

If $0 < \rho < 1$, the system is improving (happy system)

If $\rho = 1$, the failure intensity function is a constant and the model can be used in a HPP process with the exponential distribution.

To account for the varying occurrence of cracks among turbines within a given family, an additional multiplicative factor, z is introduced. This term represents the heterogeneity effect which follows a well-defined distribution. In this context, the failure intensity function is expressed by (2).

$$h(t) = z_j \omega \rho t^{\rho-1} \quad (2)$$

For mathematical convenience, the gamma and inverse Gaussian distributions are the most commonly used [10]. The gamma distribution parameterized by its variance, is given in (3).

$$f(z) = \frac{1}{\Gamma(\frac{1}{\theta})} \left(\frac{1}{\theta}\right)^{\frac{1}{\theta}} z^{\frac{1}{\theta}-1} e^{-\frac{z}{\theta}} \quad (3)$$

where Γ represents the gamma function.

A. Censored data

Cracks in turbine blades are typically detected during inspections. Some turbine runners exhibit multiple blade cracks, while others show none, leading to fully right-censored data. Consider a repairable entity j that exhibits cracks on its blade at time T_{ij} . Let C_{ij} represent the censored times at which no cracks are observed. For right-censored data, define the time

$t_{ij} = \min(T_{ij}, C_{ij})$ at each visit, and the corresponding event status δ_{ij} such that [11]:

$$\delta_{ij} = \begin{cases} 1 & \text{when } T_{ij} \leq C_{ij}, t_{ij} \text{ is not censored} \\ 0 & \text{when } T_{ij} > C_{ij}, t_{ij} \text{ is censored} \end{cases} \quad (4)$$

B. Optimization of Model Parameters

The techniques used for optimizing frailty models are the maximum likelihood (ML) and the Expectation-Maximization (EM) algorithms [12]. The ML function enhances the probability that the optimal model parameters will be obtained.

Let j be a repairable entity with a finite number of failures n_j , for $j = 1, 2, \dots, m$ turbine runners in the family. The conditional likelihood function for the entity j is expressed in (5).

$$L_j(h_0(t_{ij})|z_j) = \left[\prod_{i=1}^{n_j} (z_j h_0(t_{ij}))^{\delta_{ij}} \right] \dots \times \exp[-z_j (H_0(\tau_j) - H_0(S_j))] \quad (5)$$

where $H_0(t)$ is the cumulative hazard function defined in (6).

$$H_0(t) = \omega t^\rho \quad (6)$$

τ_j and S_j represent respectively the last and the initial times of the observation for the component j . Let assume that $S_j = 0$ day as initial time. The cumulative number of events over the time is formulated as:

$$H_j(t) = z_j \omega t^\rho \quad (7)$$

The marginal likelihood function for this component with respect to z_j is defined in (8).

$$L_j(\theta|h_0(t_{ij})) = \int_0^\infty \left[\prod_{i=1}^{n_j} (z_j h_0(t_{ij}))^{\delta_{ij}} \right] \dots \times \exp(-z_j H_0(\tau_j)) f(\theta|z_j) dz_j \quad (8)$$

Using the gamma function properties, it can be demonstrated that the marginal likelihood function is

$$L_j(\omega, \rho, \theta) = \frac{\left[\prod_{i=1}^{n_j} (h_0(t_{ij}))^{\delta_{ij}} \right] \Gamma(d_j + \frac{1}{\theta}) \theta^{d_j}}{\Gamma(\frac{1}{\theta}) [\theta H_0(\tau_j) + 1]^{(d_j + \frac{1}{\theta})}} \quad (9)$$

where $d_j = \sum_{i=1}^{n_j} \delta_{ij}$.

Equation (9) considers the frailty effect, censored data and the NHPP for repairable components. A similar expression is provided in other works without incorporating censoring [10]. In the context of inspections of turbine runners, the last visit time τ_j could vary significantly among different entities. For m components in the system, the total marginal likelihood function L is

$$L = \prod_{j=1}^m L_j(\omega, \rho, \theta) \quad (10)$$

By applying the logarithm to the marginal likelihood function to simplify its expression, the log-likelihood function yields

$$\begin{aligned} \log(L) = & \sum_{j=1}^m \left[\sum_{i=1}^{n_j} \delta_{ij} (\log \omega + \log \rho + (\rho - 1) \log(t_{ij})) \right] \dots \\ & + \sum_{j=1}^m \left[\log \Gamma(d_j + \frac{1}{\theta}) + d_j \log(\theta) - \log(\Gamma(\frac{1}{\theta})) \right] \dots \\ & - \sum_{j=1}^m \left[(d_j + \frac{1}{\theta}) \log(\theta \omega \tau_j^\rho + 1) \right] \end{aligned} \quad (11)$$

Maximizing the log-likelihood function requires setting its gradients to zero and ensuring that the diagonal terms of the Hessian matrix are negative.

In this study, the stochastic gradient decent (SGD) algorithm is used to optimize the likelihood function, as it is a Newton-Raphson method that has given good results in the literature [10], [13]. Other optimization methods, such as Nelder-Mead, used by [14], could not converge in our case. The three gradients of the log-likelihood function are presented in [15].

The optimal parameters are identified when the gradients approach zero and the diagonal elements of the Hessian matrix are negative. To further validate the optimality of the solution, the variance-covariance matrix is computed as the inverse of the Fisher information matrix. This step ensures that the variances are minimized, thereby confirming that the obtained point is indeed the optimal one. The Hessian matrix is defined as follows:

$$H = \begin{bmatrix} \frac{\partial^2 \log(L)}{\partial \omega^2} & \frac{\partial^2 \log(L)}{\partial \omega \partial \rho} & \frac{\partial^2 \log(L)}{\partial \omega \partial \theta} \\ \frac{\partial^2 \log(L)}{\partial \rho \partial \omega} & \frac{\partial^2 \log(L)}{\partial \rho^2} & \frac{\partial^2 \log(L)}{\partial \rho \partial \theta} \\ \frac{\partial^2 \log(L)}{\partial \theta \partial \omega} & \frac{\partial^2 \log(L)}{\partial \theta \partial \rho} & \frac{\partial^2 \log(L)}{\partial \theta^2} \end{bmatrix} \quad (12)$$

and the Fisher information matrix is the expected of the negative Hessian matrix such that

$$I(\omega, \rho, \theta) = E[-H(\omega, \rho, \theta)] \quad (13)$$

Therefore, the variance-covariance matrix is

$$\text{Var}(\omega, \rho, \theta) = [I(\omega, \rho, \theta)]^{-1} \quad (14)$$

The frailty term z_j has been developed by various authors. One of the approach used in this study is found in [10].

$$z_j = \frac{\frac{1}{\theta} + \sum_{i=1}^{n_j} \delta_{ij}}{\frac{1}{\theta} + \omega \tau_j^\rho} \quad (15)$$

The conditional reliability of the frailty model is given in (16).

$$R_j(t|z_j) = \exp(-z_j \omega t^\rho) \quad (16)$$

C. Confidence Interval and Model Fits

In survival analysis, assessing the reliability of a model involves examining both the confidence intervals of its parameters and how well the model fits the data. A well-fitted model ensures that the estimated distribution function closely aligns with observed data, leading to better predictions and more effective maintenance decisions [16].

The confidence interval allows for determining the uncertainty around parameter estimates, giving insight into their statistical significance. For small sample sizes, the confidence interval is typically calculated using the student's t-distribution with $k - 1$ degrees of freedom adjusted for the number of parameters [17]. The confidence interval $IC(g(\xi))$ of a function $g(\xi)$ is

$$IC(g(\xi)) = \left[g(\xi) \pm t_{\frac{\alpha}{2}, k-1} \sqrt{\text{Var}(g(\xi))} \right] \quad (17)$$

where k is the sample size, $\xi = (\omega, \rho, \theta)$ represents the estimated parameters and $\text{Var}(g(\xi))$ represents the variance of the function $g(\xi)$ such that

$$\text{Var}(g(\xi)) = \left(\frac{\partial g(\xi)}{\partial \xi} \right)^T \text{Var}(\xi) \frac{\partial g(\xi)}{\partial \xi} \quad (18)$$

where $\frac{\partial g(\xi)}{\partial \xi}$ is the vector of gradients of $g(\xi)$ defined at ξ . The variance-covariance matrix $\text{Var}(\xi)$ is defined in (14).

Several tests exist to assess the fit between a model and data. The most popular methods for evaluating the predictive accuracy of a model with a small sample size are the Root Mean Squared Error (RMSE), Akaike Information Criterion (AIC), and Chi-square test [18]. AIC is generally used to compare two different models based on their log-likelihood values.

RMSE directly compares model predictions to observed data, offering a straightforward and intuitive way to evaluate model fit using the following relation [10]:

$$\text{RMSE} = \sqrt{\frac{\sum_{i=1}^{n_j} (f_i - o_i)^2}{n_j}} \quad (19)$$

where f_i and o_i are the expected and the observed number of failures in component j . The best fit corresponds to the minimum value of the RMSE.

The Chi-square test compares the observed survival times or failure events with the expected values predicted by the model [19]. The formula for the Chi-square test statistic is:

$$\chi^2 = \sum_{i=1}^K \frac{(O_i - F_i)^2}{F_i} \quad (20)$$

where O_i , F_i represent the observed and expected frequencies, respectively, and K the number of intervals. The calculated chi-square value must be less than the critical value at the chosen level of significance, typically 95%.

Another comparison made in this work is between the cumulative hazard function and the Nelson-Aalen estimator,

which is a non-parametric model for censored data. Let $N(t)$ be number of events occurred by time t . The Nelson-Aalen estimator is

$$\hat{H}(t) = \sum_{i:t_i \leq t} \frac{d_i}{n_i} \quad (21)$$

where t_i is the event time for the i -th observation. d_i is the number of event at time t_i and n_i is the number of individuals at risk before t_i .

III. DATA AND SIMULATIONS

Data used in this study comes from 18 similar Francis turbines. The turbines are classified into two different families (D and E) based on the material of manufacturing. Family D has blades, crown, and band made of ASTM A27 carbon steel and Family E has blades made of CA6NM stainless steel and, crown and band made of A27 carbon steel. Tables I and II present the time and status events for turbine runners in family D. Tables III and IV present the time and status events for turbine runners in family E.

TABLE I
EVENT TIMES FOR TURBINE RUNNERS IN FAMILY D (DAYS).

GR 03	GR04	GR14	GR19	GR23
100	365	5110	365	7300
5475	7665	5840	6935	8760
6935	8030	6205	7665	9855
8395	8760	8760	10220	11680
11680	9855	11315	11680	14965
12410	11680	13505	14235	
14965	12045	15330		
	15695			

TABLE II
EVENT STATUS FOR TURBINE RUNNERS IN FAMILY D.

GR 03	GR04	GR14	GR19	GR23
1	1	1	1	1
1	1	0	1	0
1	0	1	0	0
1	1	0	0	1
1	1	1	0	0
0	1	1	0	
1	0	1		
	1			

All turbine runners have 13 blades, each exhibiting distinct characteristics. Optimization is performed using the gradient descent algorithm, with the learning rate and initial parameters chosen to obtain the optimal values of parameters that satisfy the conditions outlined in Section II-B.

Optimal parameters, their corresponding variances, and the maximum value of the log-likelihood are presented in Table V.

IV. RESULTS AND DISCUSSION

The simulation results revealed significant variability in the cracking behavior of turbine runners for both families, as

indicated by the variance θ in Table V. Family E appears to be more reliable, based on the value of ρ . The frailty values, calculated using the formula in (16) are presented in Fig. 2 and 3, respectively, for families D and E. Turbine runners with higher frailty values, such as GR01, GR03, GR04, and GR25, are expected to experience a higher number of cracking events. In contrast, turbine runners GR06, GR07, GR08, and GR09 exhibit nearly identical frailty values, making it efficient to select just one of them as a representative model. This approach could help in reducing the number of inspections and optimize the maintenance strategy. The same strategy could be applied to GR19 and GR23 in family D.

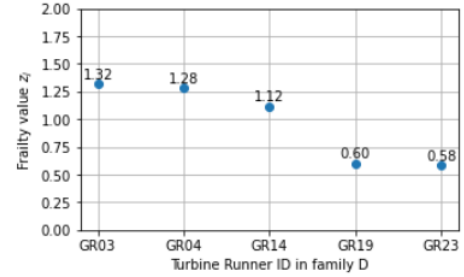


Figure. 2. Frailty Values for Turbines in Family D

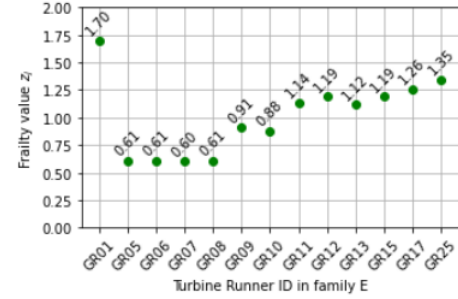


Figure. 3. Frailty Values for Turbines in Family E

The reliability curves for both families are shown in Fig. 4 and Fig. 5, respectively. In these figures, these turbine runners demonstrate similar reliability.

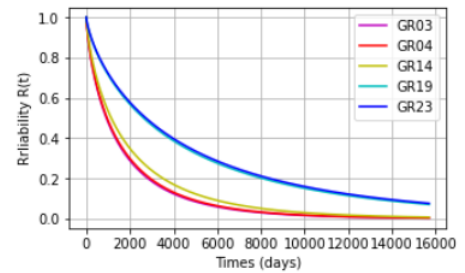


Figure. 4. Reliability Function for Turbines in Family D

A comparison at 6,000 days shows that the turbine runners GR05, GR06, GR07, GR08, GR19, and GR23 have a reliability above 0.2. A comparison at 16,000 days demonstrates that

TABLE. III
EVENT TIMES FOR TURBINE RUNNERS IN FAMILY E (DAYS).

GR 01	GR05	GR06	GR07	GR08	GR09	GR10	GR11	GR12	GR13	GR15	GR17	GR25
5840	1825	1825	2920	2190	1825	1825	3650	2920	3650	1825	5475	5475
6935	2555	2555	3650	3285	2190	2920	4380	3650	4380	2555	6205	6205
7300	3285	3285	4015	3650	2920	3650	5110	4380	5475	3285	6935	6935
8030	7300	3650	6570	6570	3650	4015	5475	4745	8030	4015	9855	7665
8395	10220	5110	8760	10200	5840	7665	6205	7300	11315	7300	11680	9490
9855		7300	10585		8030	10585	8395	9855		9855	13870	12045
12045		10220			9855		10950					
12775												
14600												

TABLE. IV
EVENT STATUS FOR TURBINE RUNNERS IN FAMILY E .

GR 01	GR05	GR06	GR07	GR08	GR09	GR10	GR11	GR12	GR13	GR15	GR17	GR25
1	0	0	0	0	1	1	1	1	1	0	1	1
1	0	0	0	0	0	0	0	0	0	1	0	1
1	0	0	0	0	0	0	0	0	0	0	0	0
0	0	0	0	0	0	0	1	0	1	0	1	0
0	1	0	0	1	0	0	0	1	1	1	1	1
0		0	1		0	1	0	1		1	1	1
1		1			1		1					
1												
1												

TABLE. V
OPTIMAL MODEL PARAMETERS.

	ω	ρ	θ	$\text{var}(\omega)$	$\text{var}(\rho)$	$\text{var}(\theta)$	$\log(L_{max})$
family D	0.0032	0.75	0.86	4.01e-5	3.9e-2	2.71e-2	-196.33
family E	0.0043	0.68	0.85	1.93e-5	1.13e-2	1.40e-2	-331.41

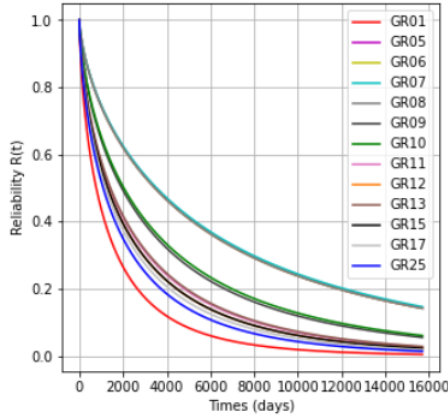


Figure. 5. Reliability Function for Turbines in Family E

most turbine runners in family E are more reliable than those in family D. Therefore, the material alone does not appear to be the sole factor contributing to the variability in cracking.

An example of comparison of the cumulative hazard function $H(t)$ curves from the frailty model, the cumulative number of failures $N(t)$, and the Nelson-Aalen estimator $\hat{H}(t)$ for turbine runner GR11 is presented in Fig. 6. It can be observed that the results from the parametric model provide

more accurate estimates of crack events compared to the non-parametric models for censored data. The confidence intervals for the $H(t)$ function, calculated using the delta method, are wider due to the limited amount of data. Alternative techniques, such as the bootstrap method, could be employed to better estimate the uncertainty, as the cumulative hazard function is not linear.

RMSE calculations and comparisons between the frailty model and the Nelson-Aalen estimator indicate that, in most cases (when the number of cracks exceeds one), the frailty model provides superior predictions, as illustrated in Fig. 7. GR17 is the only exception. Nonetheless, the Nelson-Aalen estimator consistently underpredicts the occurrence of cracks compared to the frailty model for all turbines. Moreover, using a 95% significance level, the chi-squared test indicated that the frailty model can be accepted despite the limited data, as illustrated in Fig. 8.

V. CONCLUSION

Hydraulic turbine runner blade cracking is a rare event, resulting in right-censored and limited data. The use of the frailty model and robust optimization method has demonstrated promising results when compared to the available data. The computed frailty terms allowed the classification of turbine runners based on their reliability evolution. This

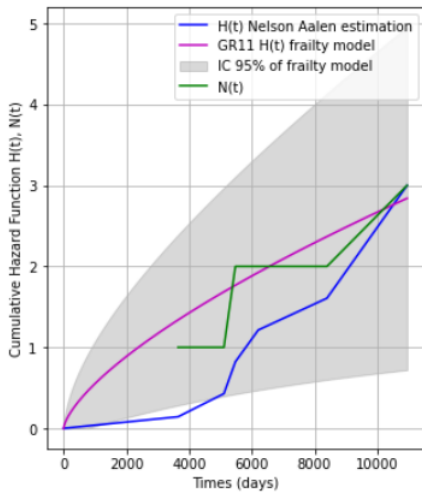


Figure. 6. $H(t)$, $\hat{H}(t)$, $N(t)$ comparison and confidence interval for GR11.

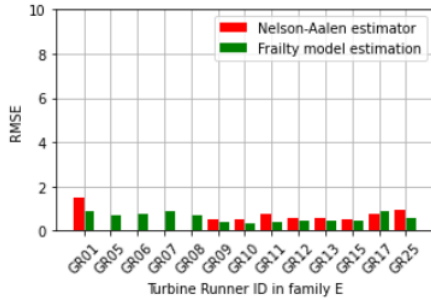


Figure. 7. Comparison of RMSE.

could be valuable in optimizing maintenance strategies by monitoring a single turbine runner as a representative model. A comparison based on the cumulative number of events revealed strong agreement between the actual and calculated values of the cumulative failure function. When compared to the Nelson-Aalen estimator using root mean squared error, the frailty model demonstrated superior accuracy. Moreover, a chi-square test at the 95% significance level confirmed that the model is acceptable despite the limited dataset. A confidence interval based on the estimated cumulative hazard function, using the

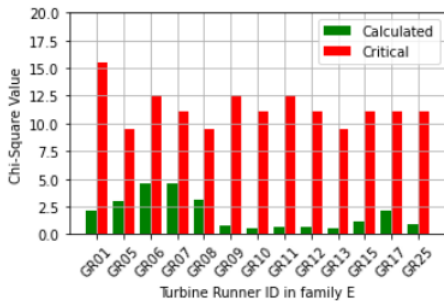


Figure. 8. Chi-square Test Comparison of Model Predictions.

delta method, yielded a large interval that encompasses the true cumulative number of events. Other techniques can be used to calculate the uncertainty in the estimation of this function.

While challenges remain, such as the complexity of the model's expressions and the derivation of the likelihood function, the careful selection of initial parameters and optimization criteria have contributed to more accurate estimates. Future research could focus on incorporating explanatory variables to enhance its predictive and interpretive capabilities.

REFERENCES

- [1] Gielen, Dolf, et al. "The role of renewable energy in the global energy transformation." *Energy strategy reviews* 24 (2019): 38-50.
- [2] Karna, Aaditya, et al. "A review of condition monitoring in Francis turbines for predictive maintenance." *Journal of Vibration and Control* (2025).
- [3] Trivedi, Chirag, et al. "Experimental investigations of transient pressure variations in a high head model Francis turbine during start-up and shutdown." *Journal of Hydrodynamics* 26.2 (2014): 277-290.
- [4] Gagnon, M., Tahan, A., Bocher, P., Thibault, D. "On the stochastic simulation of hydroelectric turbine blades transient response. Mechanical systems and signal processing" (2012), 32, 178-187.
- [5] Morin, Olivier, Denis Thibault, and Martin Gagnon. "On the comparison of hydroelectric runner fatigue failure risk based on site measurements." *IOP Conference Series: Earth and Environmental Science*. Vol. 774. No. 1. IOP Publishing, (2021), Lausanne.
- [6] Wen, Yuxin, et al. "Recent advances and trends of predictive maintenance from data-driven machine prognostics perspective." *Measurement* 187 (2022): 110276.
- [7] Balan, Theodor A., and Hein Putter. "A tutorial on frailty models." *Statistical methods in medical research* 29.11 (2020): 3424-3454.
- [8] Slimacek, V., Lindqvist, B. H. "Reliability of wind turbines modeled by a Poisson process with covariates, unobserved heterogeneity and seasonality". *Wind energy* (2016), 19(11), 1991-2002.
- [9] KDias De Oliveira, Maristela, Enrico A. Colosimo, and Gustavo L. Gilardoni. "Power law selection model for repairable systems." *Communications in Statistics-Theory and Methods* 42.4 (2013): 570-578.
- [10] Brown, Bodunrin, et al. "Reliability evaluation of repairable systems considering component heterogeneity using frailty model." *Proceedings of the Institution of Mechanical Engineers, Part O: Journal of Risk and Reliability* 237.4 (2023): 654-670.
- [11] Guo, Jinxin, et al. "Jointly modeling responses and omitted items by a competing risk model: A survival analysis approach." *British Journal of Mathematical and Statistical Psychology* (2025).
- [12] Li, Lu, et al. "Bivariate degradation modeling and reliability analysis based on generalized nonlinear Wiener processes and a shared frailty factor." *Quality and Reliability Engineering International*, (2024).
- [13] Dagal, Idriss, et al. "Adaptive Stochastic Gradient Descent (SGD) for erratic datasets." *Future Generation Computer Systems* 166 (2025): 107682.
- [14] Munda, M., Rotolo, F. and Legrand, C. (2012). parfm: Parametric frailty models in R. *Journal of Statistical Software*, 51, 1-20.
- [15] Tshibangu, Théophile Mbuyi, et al. "Reliability Analysis of Francis Turbine Cracking Using Gamma Frailty Model and Censored Historical Maintenance Data." *Sciences and Technology Publications*, (2024).
- [16] Allison, Paul D. *Survival analysis using SAS: a practical guide*. Sas Institute, (2010).
- [17] Ragni, Alessandra, Giulia Romani, and Chiara Masci. "TimeDepFrail: Time-Dependent Shared Frailty Cox Models in R." 2501.12718 (2025).
- [18] West, Stephen G., Aaron B. Taylor, and Wei Wu. "Model fit and model selection in structural equation modeling." *Handbook of structural equation modeling* 1.1 (2012): 209-231.
- [19] Radwan, O., et al. "Leveraging Weibull Analysis and Python Automation for Enhanced Failure Prediction of Electrical Submersible Pumps." *Mediterranean Offshore Conference. SPE*, (2024).